CHINESE GEOGRAPHICAL SCIENCE
Volume 7, Number 3, pp.278-288, 1997
Science Press, Beijing, China

ESTIMATION OF VEGETATIVE SURFACE ALBEDO IN THE KUSHIRO MIRE WITH LANDSAT TM DATA
——A New Approach to Atmospheric and Spectral Corrections

Zhao Wenjing(赵文经)　Hidenori TAKAHASHI
Graduate School of Environmental Earth Science, Hokkaido University, Sapporo, 0060 *Japan*
Zhao Huanchen(赵焕宸)
Changchun Institute of Geography, the Chinese Academy of Sciences, Changchun 130021, *P.R. China*
(Received 28 October 1996)

ABSTRACT: A method has been developed for estimating the filtered narrow band surface albedo with Landsat/TM data. In this method, the surface albedo from filtered range of Landsat/TM is converted to the surface albedo with unfiltered spcectral range. The atmospheric effects on each channel are systematically different, because of the different spectral behavior of atmospheric parameters. As a result, in this study, atmospheric correction has been done respectively in different parameters for visible and infrared channels. The surface albedos of the Kushiro Mire gotten with this method were compared with the observed data there. The results show that the satellite inferred albedos have a good agreement to the diurnal mean of ground observed albedos with 3% systematic error. There is a seasonal variation of albedo in high and low mires, the albedo decreased gradually from April to July and reached its minimum in July, further it rose gradually from August to October. It is also clear that there is a characteristic pattern of surface distribution according to the vegetation types of this area. The average surface albedos of each type of community are 0.164 for *Sphagnum*, 0.175 for *Carex*, 0.179 for *Pragmites* and 0.166 for *Alnus*. In the other words, the albedo in high mire (mainly covered by Sphagnum) is lower than that in low mire (mainly covered by *Phragmites* and *Carex*).
KEY WORDS: mire vegetation, surface albedo, Landsat images, remote sensing

I. INTRODUCTION

Nowadays, the remote sensing techniques have been applied in meteorology, oceanography, hydrology and some other scientific fields, and become a useful method for monitoring a vast region. Monitoring with satellite remote sensing has many advantages in collecting data continuously, regularly and repeatedly in a large area, in particular in a vast wetland where the field investigation is very difficult. Therefore, remote sensing with satellite data is the most suitable method for the survey in this kind of region.

Until the middle of the 20th century, wetland has sometimes been recognized as wasteland. However, they have many influences on the surrounding environments and are so called a great treasure house for wild animals and plants. The micro and local climate in wetland is strongly related to heat and water balance, plant growth and ground water condition of the wetland. Moreover, the vegetation albedo of wetland is not only one important parameter for estimating the heat and water balance on the surface of mire, but also has close relationship with ground water level. Therefore, it is very useful to make clear the distribution of the vegetative albedo in the mire. For the sake of atmospheric correction from satellite data, a linear relation between a clear-sky planetary albedo and surface albedo was developed by Chen and Ohing (1984) based on Lacis and Hansen's (1974) parameterization. This relation was modified by Nakagawa (1992) for NOAA AVHRR data in Antarctica, and for Landsat MSS data in Shizuoka Prefecture to obtain the filtered surface albedo from the filtered planetary albedo. The atmospheric effects on each satellite channel are systematically different, because of the different spectral behaviors of atmospheric parameters. As a result, in this study, atmospheric correction has been done respectively in different parameters for visible and infrared channels.

Tani (1990) estimated evapotranspiration and heat balance in a agricultural land and a forest area with NOAA AVHRR data applying the method of spectral correction which was based upon the atmospheric transmittance/radiance model (Kneyzys *et al.*, 1980). In this study, the coefficients are modified to be suitable for Landsat TM data.

The purpose of this study is to develop a new method for estimating the unfiltered surface albedo with Landsat To data, and to analyze the vegetative abledo distribution in the Kushiro Mire. Further, the albedo estimated from satellite data was compared with the albedo observed in the mire using albedo meter.

II. REGIONAL DESCRIPTION

The Kushiro Mire is located near Kushiro City in the East Hokkaido, and faces to the Pacific Ocean in the south of the mire. The other three sides of the mire are surrounded by steep slopes of hills and marine terraces that are lower than 140 m. Configuration of the mire is very complex because the fringes expand outward along the rivers. The main area of the mire is 10 – 13 km in the latitudinal direction and about 18 km in the longitudinal direction (Fig. 1). Land surface of the Kushiro Mire is very flat and the altitude is lower than 10 m above mean sea level in whole area.

The climate of Kushiro area is characterized by its low annual mean temperature of 5.5 ℃, which is the lowest one in all meteorological stations in Japan except the Mt. Fuji Weather Station. The sunshine rate in summer (June to August) is the lowest in Japan, caused by adventive fog that originates from the Kurile Current. The annual total precipitation is 1104

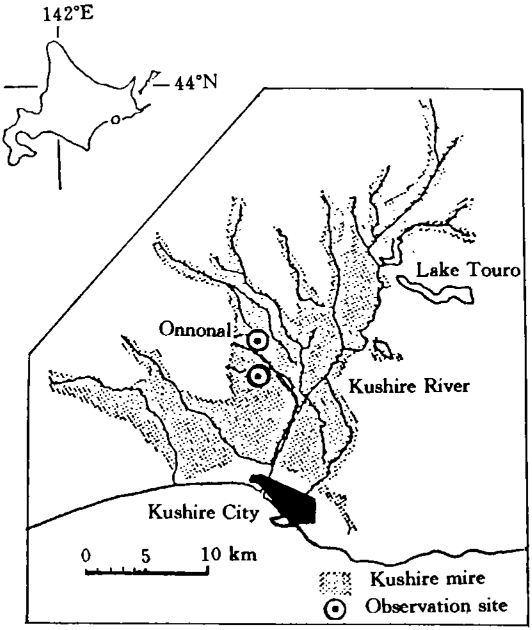

Fig. 1 Location of the Kushiro Mire and studied site

mm and 67% of it falls in the warm season (May to October). Mean maximum depth of snow cover is 43.8 cm, which is a half depth of that in the coast area of Japan Sea. The maximum depth of frozen soil reaches 50 cm in winter.

III. METHODS

On the principle of this study, the field observation and satellite observation must be carry out at the same time. The field observations were carried out from 24 June to 4 August 1993 and from 24 April to 31 December 1994 respectively. The Lansat TM data of 21 May 1984 and 1 July 1993 were analyzed, because the foggy and cloudy weather limited the remote sensing.

The flow chart of analysis is shown in Fig. 2. In order to make the program be simple and fast one, the geometric processing was done as the first step.

There are many influences of absorption and scattering by gas molecules on radiation along the path through the atmosphere from the top of atmosphere to satellite after reflecting on the earth surface. Atmosphere corrections are very important to get good results from satellite data.

It is also very necessary to do narrow-to-broad band conversion in order to derive the broad band albedo from the satellite measured data. Thus the spectral correction was done after atmospheric correction.

The field data were also analyzed to consider the relation of the surface albedo to precipitation and groundwater condition.

1. Method for Atmospheric Correction

The solar radiation absorption model is described by Lacis and Hansen (1974). In their approach, absorption of solar radiation is parameterized as a function of water vapor distribution, zenith angle of the sun, albedo of the earth surface and ozone distribution. It is considered that the water vapor absorption is significant at the wavelength region longer than 0.7μm, and that ozone absorption and Rayleigh scattering are significant at the rest of wavelengths. However, in Nakagawa's paper, the atmospheric correction has been done, but on the one hand the water vapor absorption, ozone absorption and Rayleigth scattering were only included in final regression formula together, on the other hand filtered range of Landsat TM channels is 0.45 –

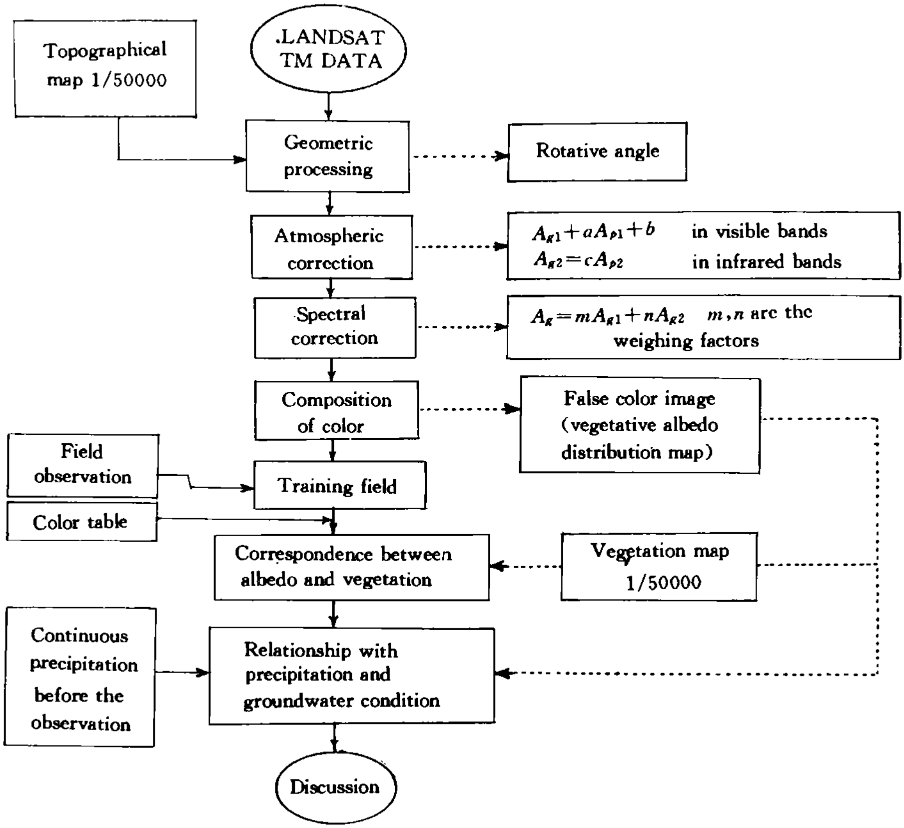

Fig. 2 Flow chart of analysis

2.35μm (bands 1 – 5 and 7), which are included both in visible and infrared bands, and it has been fully proved that the optical effects of atmosphere in visible and infrared bands are different from each other (Koepke, 1989). Therefore, in this paper, the filtered range of Landsat TM channel 1 – 5 and 7 were divided into two parts, i.e. the part Ⅰ which is the wave region longer than 0.7μ m (channels 1,2 and 3) and the part Ⅱ which is the rest wave regions (channels 4,5 and 7). The different atmospheric corrections were done for parts Ⅰ and Ⅱ, respectively.

The filtered planetary albedos A_{P1} and A_{P2} have been obtained for the wave regions: parts Ⅰ and Ⅱ, respectively, by the following formula:

$$A_{P1} = \frac{\{1 + 0.0167 \sin [2\pi(J - 93.5)/365]\}^2 \pi \sum_i R_i}{1382 \times 0.2713\mu} \quad (i = 1,2,3) \tag{1}$$

$$A_{P2} = \frac{\{1 + 0.0167 \sin [2\pi(J - 93.5)/365]\}^2 \pi \sum_i R_i}{1382 \times 0.1495\mu} \quad (i = 4,5,7) \tag{2}$$

where, μ is the sine of the solar zenith angle; and J is Julian day. The sum of the terms within the braces in Equation (1), (2) is the correction for the distance between the sun and earth

(Gurney and Hall, 1983).

The filtered radiative brightness in the ith wavelength region R_i is estimated from the Landsat TM data. R_i is given by the following formula:

$$R_i = \frac{V}{D_{\max}}(R_{\max} - R_{\min}) + R_{\min} \tag{3}$$

where, $D_{\max}=255$ for TM; V is digital data which got from CCT, and its geometric correction has been done. $R_{\max}$ and $R_{\min}$ are the maximum and minimum radiative brightness come from displacement sensor, respectively.

In order to obtain the surface albedo from the planetary albedo, the methods of Chen and Ohing (1984) and Nakagawa (1992) were developed in the present study. Lacis and Hansen's (1974) parameterization was also used in the atmospheric correction. Since Lacis and Hansen's (1974) parameterization expresses the ozone and water vapor absorptivity and the Rayleigh albedos in units of the total solar constant, it is necessary to convert this parameterization from unfiltered spectral range to the filtered ranges for parts Ⅰ and Ⅱ. According to Thekaekara and Drummond (1971), the ratios of the filtered solar constant in the wave regions for parts Ⅰ and Ⅱ to the total solar constant are 0.2713 and 0.1495, respectively. Therefore, in order to express such parameters in units of the filtered solar constant, the original parameters of Lacis and Hansen (1974) were divided by 0.2713 and 0.1495 for parts Ⅰ and Ⅱ, respectively, for excluding the contributions outside of these wavelengths.

According to Lacis and Hansen's parameterization, the major absorbers in the earth-atmosphere system are ozone in the stratosphere (the wavelength regions for part Ⅰ), water vapor in the troposphere (the wavelength regions for part Ⅱ) and the earth surface. The absorptance of those are given by

$$TA_{O3} = A_{O3}(x)\{R_a + \frac{(1-R_a)(1-R_a^*)A_{g1}}{1-R_a^*A_{g1}}\} \times \{A_{O3}(x^*) - A_{O3}(x)\} \tag{4}$$

$$TA_w = A_w(y) + A_{g2}[A_w(y^*) - A_w(y)] \tag{5}$$

and the fractions of the filtered solar constant absorbed at the earth surface in the spectral regions for parts Ⅰ and Ⅱ (TA_{g1} and TA_{g2}, respectively) are given by the following formulas:

$$TA_{g1} = \frac{\{1 - R_r - A_{O3}(x)\}(1 - A_{g1}}{(1 - R_r^* A_{g1})}] \tag{6}$$

$$TA_{g2} = [1 - A_w(y)](1 - A_{g2}) \tag{7}$$

where $A_{g1}$and A_{g2} are the filtered surface albedos in the spectral regions for parts Ⅰ and Ⅱ of Landsat TM, respectively, and x and y are the total atmospheric ozone and water vapor path lengths traversed by the direct solar beam for reaching the earth surface, respectively, which are given by

$$x = \mu M \tag{8}$$

$$y = wM \tag{9}$$

x^* and y^* are the total path lengths of ozone and water vapor traversed by the reflected radiation in reaching the top of the atmosphere , respectively , and x^* and y^* are given by

$$x^* = u(M + 1.9) \tag{10}$$

$$y^* = w(M + 5/3) \tag{11}$$

where $M\ (=35/\sqrt{(1224\ \mu^2+1)})$ is the optical air mass, u is the total ozone amount (atm-cm), w is the effective water vapor content (cm) which is estimated from air temperature T_0(°K), air pressure P_0(hPa) and water pressure e_0(hPa) by the following formula (Nakagawa, 1988):

$$w = \frac{0.0351 e_0 P_0}{T_0} \tag{12}$$

A_{o3} is given by the following formula, which is modified based on Lacis and Hansen (1974) parameterization:

$$A_{o3} = \frac{0.02118x}{(1 + 0.042x + 0.000323x^2) \times 0.2713} \tag{13}$$

According to Lacis and Hansen's (1974) parameters, the absorption bands of water vapor were considered to be in the band range of 0.7 – 4.0 μm. However, the band range part Ⅱ of Landsat TM is composed only of 0.76 – 0.96 μm (channel 4), 1.55 – 1.75 μm (channel 5) and 2.08 – 2.35 μm (channel 7). Thus in this study, it is necessary to subtract the water vapor absorption of the remaining range in part Ⅱ from Lacis and Hansen's (1974) parameters. Empirical constants for water vapor absorption bands were described by Liou and Sasmori (1975) based on the study of Howard *et al*. (1956).

The principal bands which are absorbed by water vapor in the infrared region were compiled by Goody (1964) from various sources. Since only part of bands 4,5 and 7 stands in these bands, in the other words, the effects of water vapor absorption only occurred in these regions for this study. And in Lacis and Hansen (1974) parameterization, the effects of water vapor absorption bands in all spectra were subtracted. Thus, it is necessary to remove the contributions outside of bands 4, 5 and 7.

As a result, the water vapor absorption correction A_w is given by following formula:

$$A_w = \frac{2.9y \times 0.1495}{[(1 + 141.5y)^{0.635} + 5.925y]} - \frac{\sum [C_i + D_i \log_{10}(y \times P^{K_i/D_i} + 10^{-\frac{C_i}{D_i}})] \times 0.1495}{\triangle_{vi} \times BR_i} \tag{14}$$

where y is the optical path length, p is the air pressure, C, D and k are empirical constants given by Liou and Sasamori (1975), $\triangle_{vi}$ is wave number in each absorption band, and also given by Liou and Sasamori (1975), BR_i is the percentage of solar radiation in each water vapor absorption bands for bands 4,5 and 7.

The Rayleigh albedo of the total atmosphere for the incoming solar radiation flux, R_r, in parameterized form, is given by

$$R_r = \frac{0.28 \times 0.2653}{(1 + 6.43\mu_0) \times 0.2713} \tag{15}$$

and the spherical albedo of the total atmosphere for the radiation from below, R_r^* can be written as

$$R_r^* = \frac{0.0658 \times 0.2653}{0.2713} \quad (16)$$

The Rayleigh albedo of the atmosphere underlying the ozone layer for the incoming solar radiation flux, R_a, in parameterized form, is given by

$$R_a = \frac{0.217}{(1 + 0.816\mu_0 \times 0.2713} \quad (17)$$

and the spherical albedo of the atmosphere underlying the ozone layer for radiation from below, $R^* a$, is written as

$$R_a^* = \frac{0.144 \times 0.2653}{0.2713} \quad (18)$$

The number 0.2653 is the percentage of Rayleigh scattering intensity between 0.45 − 0.69 μm (channels 1,2 and 3) estimated from Thekaekara and Drummond (1971).

In the wavebands parts Ⅰ and Ⅱ of the Landsat TM, subtract $TA_{O3}$and TA_{g1}, TA_w and $TA_{g2}$from unity, respectively, the relationships between the filtered planetary albedos A_{p1} (part Ⅰ), A_{p2}(part Ⅱ) and the filtered surface albedos A_{g2}(part Ⅱ) are expressed respectively as follows:

$$A_{p1} = 1 - A_{O3}(x) - R_a[A_{O3}(x^*) - A_{O3}(x) - \frac{1 - R_r - A_{O3}(x)}{(1 - R_r^* A_{g1})}$$
$$+ \{\frac{1 - R_r - A_{O3}(x)}{(1 - R_r{}^* A_{g1})} + \frac{(1 - R_a)(1 - R_a^*)}{1 - R_a^* A_{g1}} \times [A_{O3}(x^*) - A_{O3}(x)]\} A_{g1} \quad (19)$$

$$A_{p2} = [1 - A_w(y^*)]A_{g2} \quad (20)$$

In equations (19) and (20) the filtered planetary albedos were simulated from a variety of filtered surface albedo, surface air temperature, surface atmospheric pressure, surface water vapor pressure, total ozone amount, and solar elevation. Fig. 3 shows an example of the relationship between the planetary and surface albedos, predicted by equations (19) and (20) under the climatic conditions on 1 July 1993 at the Kushiro Mire i.e. $T_0 = 282.7$°K, $e_0 = 10.2$ hPa, $P_0 = 1008.9$ hPa, $u = 0.36$ atmcm and the solar elevation is 58°. It is very clear that the planetary albedo is linear to the surface albedo both for parts Ⅰ and Ⅱ, and these regression equations line are given by

$$A_{g1} = 1.123144A_{p1} - 0.03125 \quad (21)$$

$$A_{g2} = 1.0278A_{p2} \quad (22)$$

where, the parameter of surface air temperature, surface atmospheric pressures, surface water vapor pressures, total ozone amounts are assumed to be the same as those at the Kushiro Mire through thewhole region.

2. Method for Spectral Correction

As the last procedure, the unfiltered surface albedos must be obtaind by the spectral correction

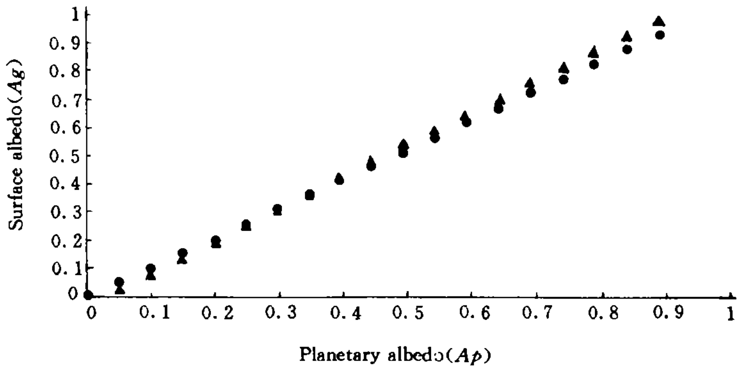

▲ $A_{g1} = 1.12314 A_{p1} - 0.03125$ ● $A_{g2} = 1.0278 A_{p2}$

Fig. 3 The relationship between the planetary and surface albedo

against the filtered surface albedos. In the present study, the spectral correction was done by the modified Kneyzys's (1980) method. Under the assumption described above, the unfiltered surface albedos can be estimated with weighted average of the parts Ⅰ and Ⅱ. The weighted average was obtaind by applying radiation transmission model's LQWTRAN6 (Kneyzys *et al.*, 1980). In the other words, the radiation energy of the wave region longer than 0.7μm and shorter than 0.7μm can be obtained by LOWTRAN6, so the ratios of both radiation energy in the unfiltered wavelength region can be derived. As a result, the regression formula of the spectral correction is giver by the following formula:

$$A_g = 0.673 A_{g1} + 0.327 A_{g2} \tag{23}$$

IV. RESULTS AND DISCUSSION

1. Results of Field Observation

The comparison of surface albedo between the high and low mires was done (Fig. 4). The changing range of albedo in high mire is smaller than that in low mire. However, from late September to early October, the opposite result is obtained, the reason is considered that the groundwater level in the high mire was higher than the ground surface owing tothe continual precipitation and the water surface exposed to air, whereas that in the low mire was also higher than the groundwater level but high vegetation canopy concealed the water surface from albedometer. Two remarkable high values on 30 April and 1 May both in the high and low mires, caused by the snowcover in these two days.

There is a remarkable seasonal variation of albedo in high and low mires. In May and June, the height of vegetation in the Kushiro Mire is still low, the albedo is affected easily by the condition of ground surface. The albedo thus fluctuate rather larger in summer. In July

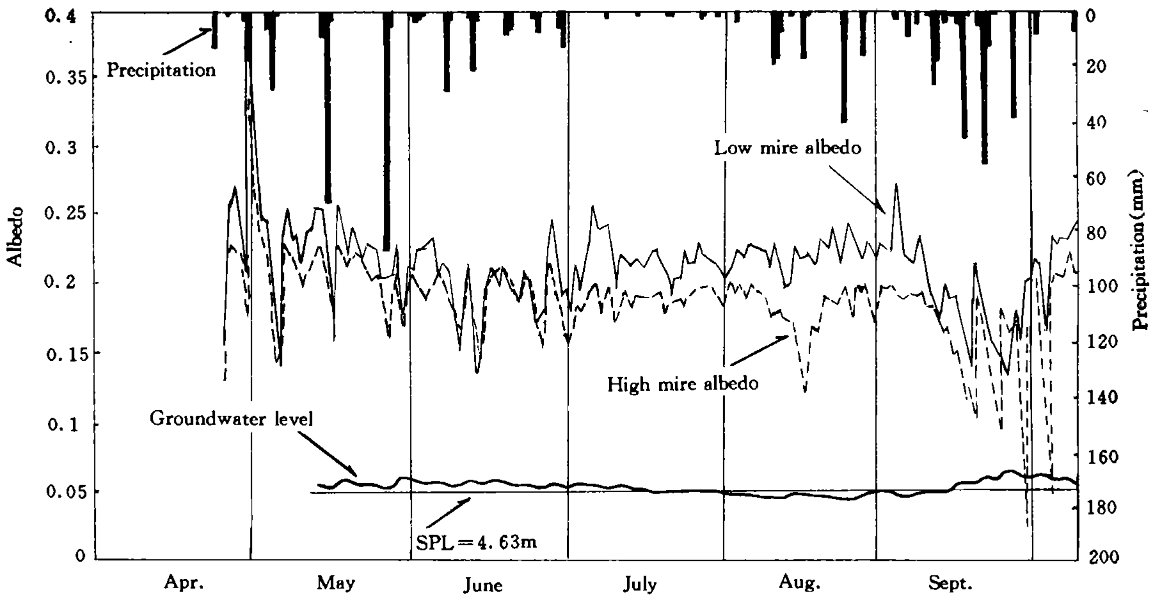

Fig. 4 The relationship among albedo, precipitation and groundwater level in high and low mires

and August, the vegetation grows luxuriantly, thus the albedo depends almost on the surface of vegetation, and the influence of the ground surface condition became very small. So the fluctuation of it was not so large. In September and October, the fluctuation of albedo is the largest because of the continual rain as described before.

Because the cloud and rain affect the albedo, it is necessary to remove these effects for consideration on seasonal variation of the surface albedo. Therefore, in this study, albedo has been got rid of when observed incidence is lower than 80% of standard radiation. The results are shown in Fig. 5. The albedo decreased gradually from April to July and reached its minimum in July, further it rose gradually from August to October.

2. Results of Estimation with Landsat TM data

To assess the reliability of the calculated value of albedo, the derived regression equation was tested through the comparison between the satellite-inferred and ground-observed values in the Kushiro Mire.

The vegetative surface albedo in the Kushiro Mire were estimated from Landsat TM data which was received on 21 May 1984 and 1 July 1993. A clear relation was seen between surfacealbedo and vegetation type. The average surface albedos of each community on 21 May 1984 are 0.199 for *Sphagnum*, 0.207 for *Carex*, 0.204 for *Phragmites* and 0.207 for *Alnus*, On 1 July 1993 are 0.164 for *Sphagnum*, 0.175 for *Carex*, 0.179 for *Phragmites* and 0.177 for *Alnus*. It is clear that the albedos of *Phragmites* and *Alnus* are larger, *Carex* is

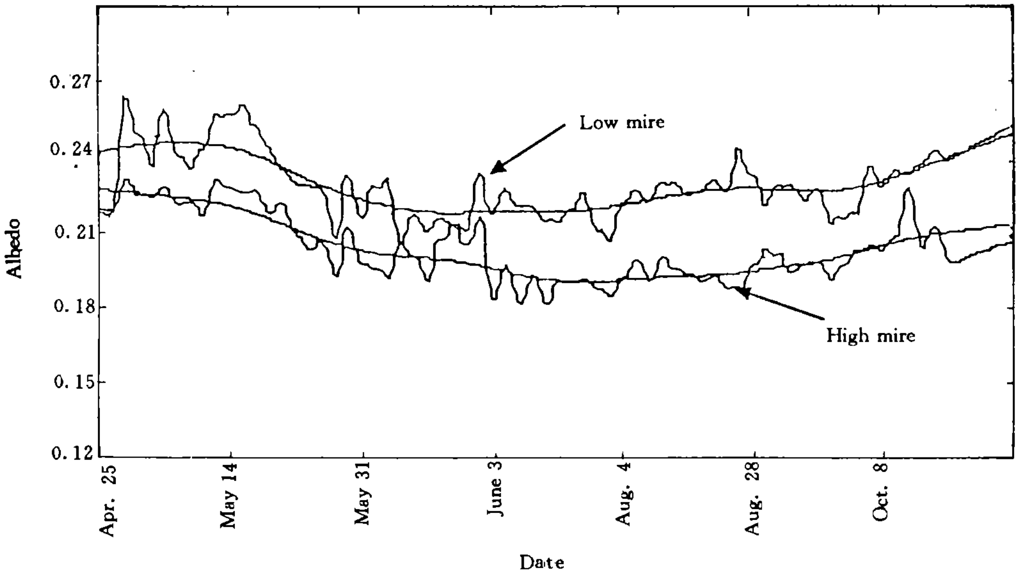

Fig. 5 Seasonal variation of albedo in high and low mires
(Fitted with the method of distance weighed least squared smoothing)

in the middle and *Sphagnum* is the smallest. This result agrees to the result of field observation. The albedo in May is higher than that in July, and this difference was also obtained from field observation.

The comparison between the estimated and observed albedos is shown in Fig. 6, On July 1, the estimated albedos agree to the observed albedos because the field observation and satellite observation were carried out at the same time, the errors are 1.09% for the high mire, 3% for the low mire. Owing to the lack of field observation on 21 May 1984, we had to compare the estimated albedo on 21 May 1984 with the observed albedo in May 1995. The result shows that the estimated albedos are all lower than the observed values, the errors are 9.05% for the high mire and 11.5% for the low mire. In order to analyze its reason, the meteorological data of snowfall in mountainous region around the Kushiro Mire was collected from November 1983 to April 1984 and from November 1993 to April 1994. The result shows that the greatest snow depth was recorded both in the two periods: 96cm at Shibecha and 55 cm at Tusrui in March 1984; 47 cm at Shibecha and 49 cm at Tusrui in March 1994. At Tusrui, the maximum snow depth was equal in the two periods, whereas at Shibecha, the maximum snowdepth in March 1984 was about twice larger than that in March 1994. This indicates that the snowmelt water inflow into the mire in May 1984 was likely to be larger than that in May 1994, and the groundwater level in May 1984 was higher than that in May 1994, accordingly. Thus the calculated albedo in May 1984 is lower than the observed value in May 1994.

ACKNOWLEDGMENTS

The authors wish to express their gratitude to Professor Kiyotaka Nakagawa of Joetsu

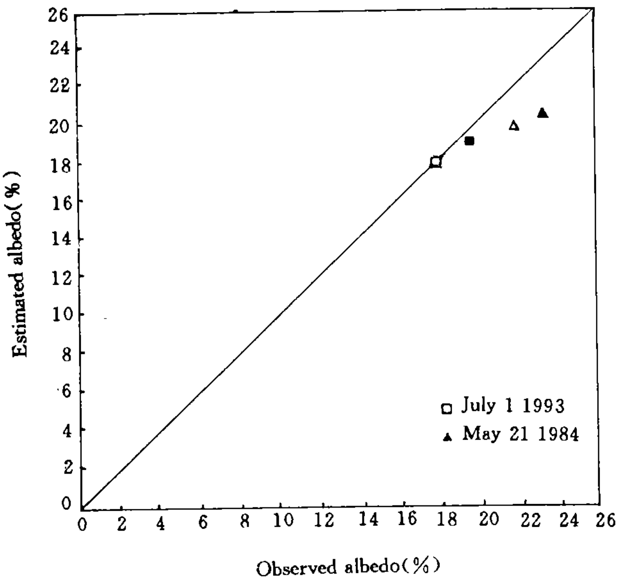

Fig. 6 The Comparison of estimated and observed values
(the white is the albedo that got from the high mire, the black is the albedo
that got from the low mire

University of Education for his invaluable advice. A special thanks for Mr. Takashi INOUE, Instructor of Faculty of Agriculture, Hokkaido University for having provided groundwater level data for testing and verifying the results of this study. Thanks also to members of Geoecological Seminar 1 of Graduate School of Environmental Earth Science, Hokkaido University.

REFERENCES

Chen T. S., Ohing G., 1984. On the relationship between clear-sky planetary and surface albedos. *J. Atmos. Sci.*, 41: 156 – 158.

Kneyzys F. X., *et al.*, 1980. Atmospheric Transmittance/Radiances; Computer Code LLOWTRANG, AFGL – TR – 83 – 0187, Air Force Geophysics Laboratory, pp. 200.

Koepke P., 1989. Removal of atmospheric effects from AVHRR albedo, *J. Appl. Meteorol.*, 28: 1341 – 1348.

Lacis A. A., Hansen J. E., 1974. A parameterization for the absorption of solar radiation in the earth's atmosphere. *J. Atmos. Sci.*, 31: 118 – 133.

Liou K. N., Sasamori T., 1975. On the transfer of solar radiation in aerosol atmospheres. *J. Atmos. Sci.*, 32: 2166 – 2177.

Liou K. N., Sasamori T., 1983. Direct determination of surface albedos from satellite imagery. *J. Climate App1. Meteorol.*, 22: 530 – 536.

Nakagawa K., 1992. Estimation of surface albedo distribution in Lutzow-Holm bay and its neighborhood with NOAA/AVHRR data.

Thekaekara M. P., Drummond A. J., 1971. Standard values for the solar constant and its spectral components. *Nature (London)*, *Phy. Sci.*, 229: 6 – 9.